ELSEVIER

Journal of Nuclear Materials 307–311 (2002) 930–934

journal of nuclear materials

www.elsevier.com/locate/jnucmat

Effect of undersized solute atoms on point defect behavior in V–A (A = Fe, Cr and Si) binary alloys studied by using HVEM

T. Hayashi *, K. Fukumoto, H. Matsui

Institute for Material Research, Tohoku University, Katahira 2-1-1, Aoba-ku, Sendai 980-8577, Japan

Abstract

Point defect behavior in pure vanadium and V–A binary alloys, which contain undersized solute atoms, are examined by using high voltage electron microscope. In alloys, the number densities of self-interstitial (SIA) loops are found to be much higher than that in vanadium, indicating that solute atoms trap SIAs and enhance loop nucleation. Moreover, in contrast to the case of pure vanadium, several stages are observed in the Arrhenius-type plot of the loop density. From the temperature dependence of the loop density in each alloy, the activation energies of 0.81, 0.65 and 0.99 eV for V–xFe ($x \geqslant 0.1$ at.%), V–yCr ($y \geqslant 1$ at.%) and V–1Si have been obtained, respectively. Complex loop shapes have been observed in all alloys. Those become more significantly with increasing solute concentration, indicating solute segregation to loops. Various observed phenomena are discussed in terms of the obtained activation energy.

1. Introduction

In order to predict material performance under irradiation environment, it is important to obtain sufficient understanding of the point defect behavior, which is often strongly affected by solute atoms. In particular, undersized solutes interact strongly with interstitial atoms (SIAs), causing microstructural and microchemical change in irradiated materials [1,2]. In order to evaluate material performance under irradiation conditions, the knowledge of fundamental parameters of point defects, e.g. the migration energies and binding energies with a solute and/or an impurity atom, is essential. Furthermore, it is also important to clarify the mechanisms of strong swelling enhancement in V–A (A: undersized solutes) binary alloys [3,4].

In this study, in situ high voltage electron microscope (HVEM) observation of SIA cluster formation and accumulation in V–A alloys under electron irradiation have been performed, in order to obtain deeper understanding of the point defect behavior and the effect of undersized solutes.

2. Experimental procedure

Vanadium of 99.9% purity, V–xFe ($x = 0.1$, 0.2, 0.3, 5 at.%), V–yCr ($y = 0.1$, 1, 5 at.%) and V–1 at.%Si were prepared. The ingots of materials were cold rolled to $\simeq 0.2$ mm thick sheets. The disks with diameter of 3 mm were punched from the sheet specimens and annealed at 1327 K in a vacuum of 2×10^{-4} Pa for 2 h. Then, the disks were thinned by electro-polishing for TEM observation.

Electron irradiation and in situ microstructural observations were carried out in HVEM (JEM ARM-1250) of High Voltage Electron Microscope Laboratory in Tohoku University at an electron acceleration voltage of 1250 kV. The irradiation temperature and electron flux were varied in the range from RT to 623 K and from 4.3×10^{22} to 3.6×10^{23} e m^{-2} s^{-1}, respectively.

* Corresponding author. Tel.: +81-22 215 2069; fax: +81-22 215 2066.

E-mail address: thayashi@imr.tohoku.ac.jp (T. Hayashi).

0022-3115/02/$ - see front matter
PII: S0022-3115(02)01162-5

3. Results

3.1. Defect behavior in V–Fe alloys

Fig. 1 shows a typical example of the microstructural evolution under irradiation. In all materials, the SIA loops were formed and grew during irradiation in a similar manner. Loop number density increased only during initial period of irradiation, and soon saturated. The behavior is typical in HVEM experiments [5,6] at low irradiation temperatures where the vacancy migration is low.

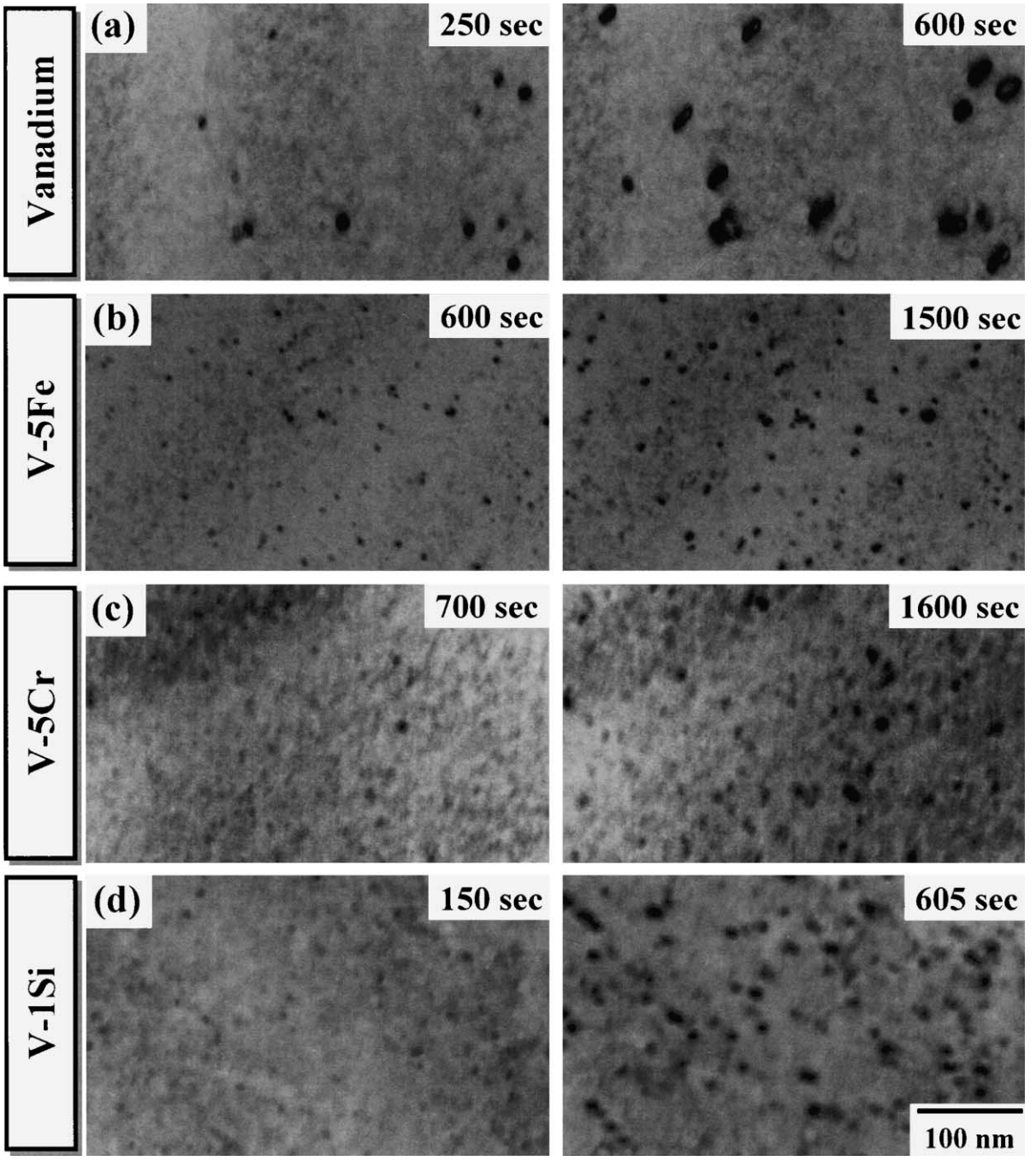

Fig. 1. Microstructural evolution in (a) vanadium, (b) V–5Fe, (c) V–5Cr and (d) V–1Si during irradiation at 393 K. Irradiated at electron fluxes of 1.1×10^{23} e m^{-2} s^{-1} (a) and 2.1×10^{23} e m^{-2} s^{-1} (b)–(d).

Fig. 2 shows the Arrhenius-type plot of measured saturated loop number density in V–xFe. As seen in the figure, the loop density in V–xFe is much higher than that in pure vanadium, indicating strong trapping of SIAs by iron atoms. In contrast to pure vanadium, in V–xFe, the temperature dependence consists of three stages; two temperature dependent stages, labeled II and IV and temperature independent stage III. According to the rate theory for the loop nucleation, proposed by Yoshida et al. [7], these stages appear when trapping of SIAs by immobile impurities is strong and trapping and detrapping of SIAs dominate loop nucleation. In stage III, impurities strongly trap SIAs and serve as the loop nucleation sites. In this case, the loop density is independent on both irradiation temperature and intensity and corresponds to the impurity concentration. In stage IV, the rate of trapping and detrapping of SIAs become comparable to that of other processes and the loop density shows temperature dependence. Assuming that di-interstitials are stable loop nuclei, the loop density is proportional to square root of irradiation intensity in this stage.

The intensity dependence in each stage has been examined in our previous study [8], where it has been shown that in V–xFe, di-interstitials are stable loop nuclei. This indicates that iron solutes strongly trap SIAs and the loop nucleation process follows the prediction of the rate theory.

3.2. Defect behavior in V–yCr

Temperature dependence of the loop number density in V–Cr is shown in Fig. 3. As seen in the figure, the loop density decreases with increasing irradiation temperature and increases with solute concentration. It can be considered that undersized chromium solutes strongly trap SIAs, thus enhancing loop nucleation. Temperature dependence in V–0.1Cr hardly changes in comparison with pure vanadium, indicating that 0.1% chromium addition does not significantly affect loop nucleation. On the other hand, in V–1Cr and V–5Cr, the temperature dependence consists of two stages, like in V–Fe alloys, i.e. the temperature independent stage III and temperature dependent stage IV.

Irradiation intensity dependence in V–yCr is shown in Fig. 4. In V–1Cr and V–5Cr, the dependence in both stages shows well agreement with the rate theory mentioned above.

3.3. Defect behavior in V–1Si

Fig. 5 shows the temperature dependence of the loop number density in V–1Si. In contrast to V–Fe and V–Cr alloys, there are two temperature dependent stages of the loop density in V–1Si. As seen in the figure, the loop density shows temperature dependence also in the lower temperature range, labeled stage III', though the de-

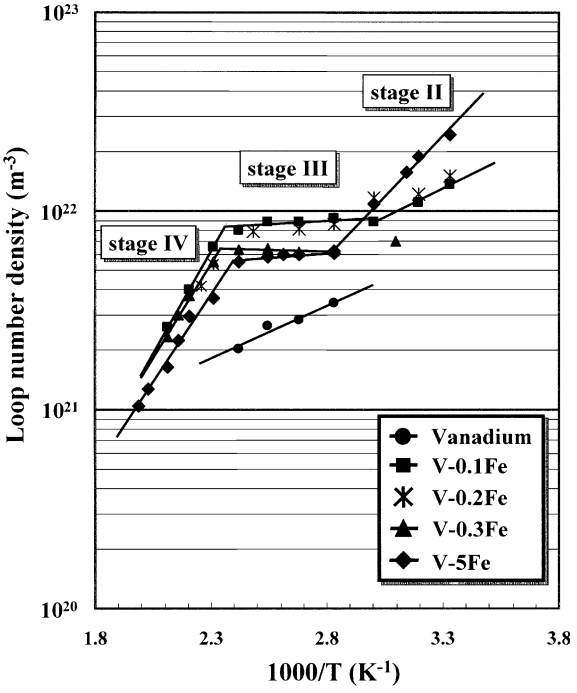

Fig. 2. Arrhenius-type plot of the loop number density in vanadium and V–Fe alloys. Irradiated at an electron flux of 2.1×10^{23} e m^{-2} s^{-1}.

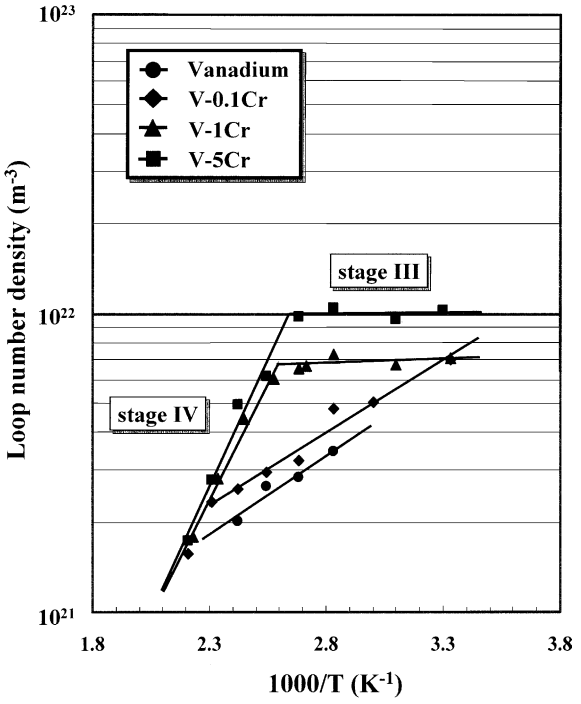

Fig. 3. Arrhenius-type plot of the loop number density in V–Cr alloys. Irradiated at an electron flux of 2.1×10^{23} e m^{-2} s^{-1}.

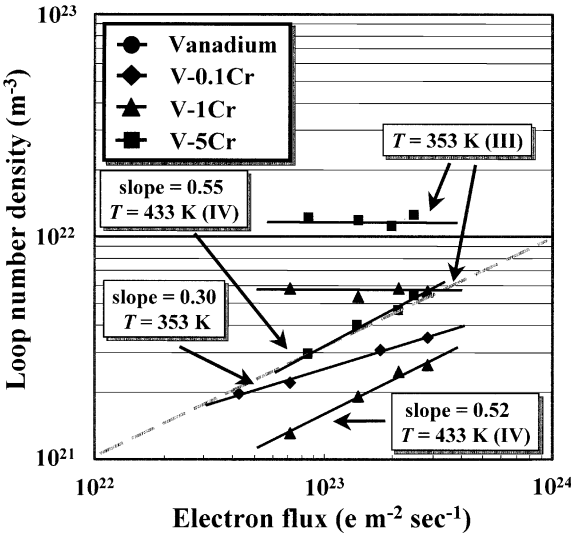

Fig. 4. Damage rate dependence of the loop number density in V–Cr. Irradiated at temperatures corresponding to each stage.

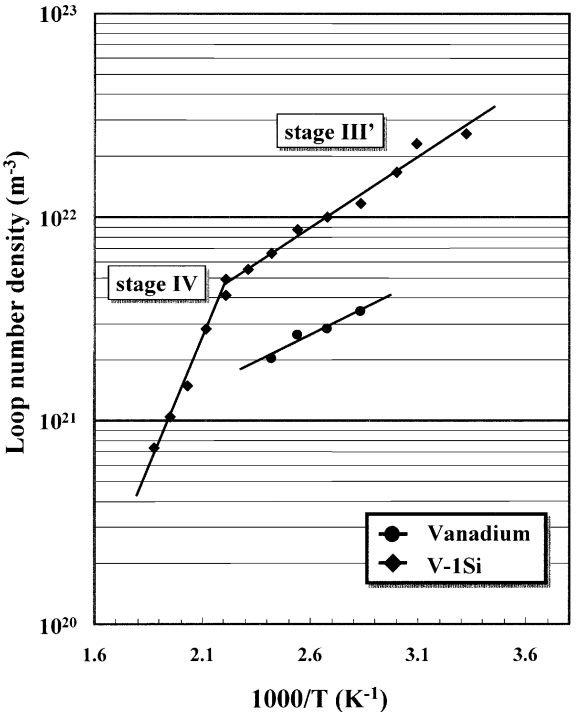

Fig. 5. Arrhenius-type plot of the loop number density in V–1Si. Irradiated at an electron flux of 2.1×10^{23} e m^{-2} s^{-1}.

pendence is weaker than that in the higher temperature stage IV. This is not the case in V–Fe and V–Cr alloys.

Intensity dependence is shown in Fig. 6. In stage IV, the loop density is proportional to the square root of irradiation intensity in good agreement with the rate theory. In stage III', however, a weaker dependence was

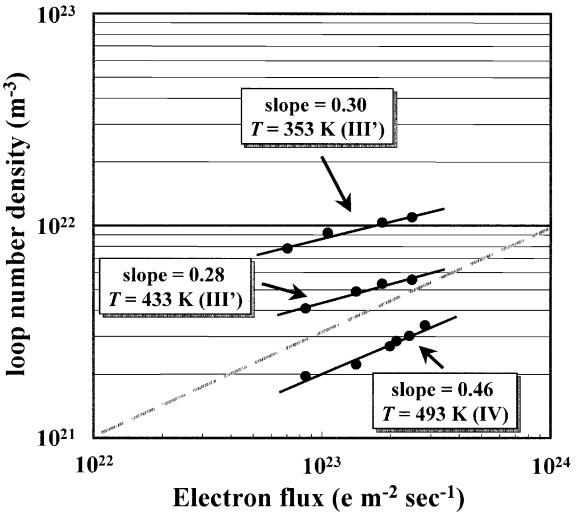

Fig. 6. Damage rate dependence of the loop number density in V–1Si. Irradiated at temperatures corresponding to each stage.

observed. This is possibly because the effect of impurities on SIA migration is not negligible in this low temperature region.

4. Discussion

4.1. Interstitial mobility in V–Fe and V–Cr

In all alloys, significant increase of the loop density was observed, indicating strong trapping of SIAs by the undersized solute atoms. Another common observation is shown in Fig. 7. Namely, the loop shapes in alloys are not smoothly roundish, but complex, like a flower with many petals. These become more significant with increasing solute concentration. Although the chemical composition of these defects could not be analyzed because of experimental difficulties, it is very likely that these were due to the solute segregation. Indeed, in previous neutron and heavy-ion irradiation experiments, same defects have been identified to be dislocations accompanied by thin solute layers [9,10]. Also in this study, in V–Fe alloy, fringe contrasts have been observed inside the dislocation loops [8]. These defects are considered to have very important role on the damage process in these alloys.

From the slopes of the lines in stage IV and using the above rate theory, the effective migration energies of a SIA of 0.81 and 0.65 eV for V–xFe ($x \geqslant 0.1$ at.%) and V–yCr ($y \geqslant 1$ at.%) have been obtained. It is interesting that the difference in the temperature dependence of loop density, i.e. the obtained activation energies, and the critical solute concentration for the appearance of the stages, can be explained qualitatively in terms of the difference in the atomic size between both solutes.

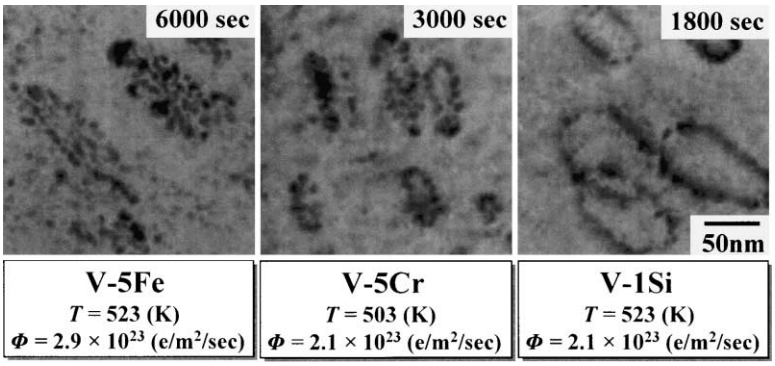

Fig. 7. Examples of the complex loop shapes observed in the alloys.

The above values are considered to represent the sum of SIA migration energy and the binding energy between a SIA and a trapping site, i.e. undersized solutes and/or interstitial impurities [7]. It is reasonable to assume that the trapping site is undersized solutes themselves because undersized solutes are considered to have strong binding with SIAs. In V–Fe alloys, however, the loop density in stage III and IV does not depend on the iron concentration, in contrast to the prediction of the rate theory. It is therefore difficult to consider that undersized solute atoms act as the direct loop nucleation sites. This indicates that undersized solutes may act as 'mobile' trapping centers in the form of the mixed or solute–solute dumbbells, which is different from the concept of the 'immobile' nucleation site in the rate theory. It is very likely that the above trapping sites in V–Fe and V–Cr are interstitial impurities.

Further study is needed to clarify 'pure' effects of these undersized solutes as mobile trapping sites. In V–Fe, in the low temperature region, it is likely that the effect of iron solutes on loop nucleation is more significant and dominates the loop nucleation, leading to the appearance of the temperature dependent stage II.

4.2. Interstitial cluster accumulation in V–1Si

In V–1Si, temperature dependence differs from those in V–Fe and V–Cr. This kind of dependence has been observed also in V–Ti alloys [11]. It is, however, difficult to explain the mechanisms dominating loop nucleation in both stages in terms of the rate theory mentioned above.

It is very likely that in the lower temperature region, the trapping by impurities is strong, and this would explain the weak dependence on irradiation temperature and intensity, observed in stage III' [12].

If it is assumed that in stage IV, the stable loop nuclei are di-interstitials and the loop nucleation process follows the rate theory, the activation energy of 0.99 eV has been obtained. In addition to the trapping and detrapping process by impurities, however, some other mechanisms could affect loop nucleation in stage IV, e.g. interaction with mobile vacancies and/or thermal decomposition of loop nuclei. Further investigations are thus needed to clarify the mechanism of the strong temperature dependence and the physical significance of the obtained activation energy.

Acknowledgements

The authors are deeply indebted to E. Aoyagi and Y. Hayasaka in High Voltage Electron Microscope Laboratory in Tohoku University for technical assistance in using HVEM. We would like to thank research foundation for the electrotechnology of Chubu for the financial support.

References

[1] L.K. Mansur, K. Farrell, J. Nucl. Mater. 170 (1990) 236.
[2] E.P. Simonen, S.M. Bruemmer, J. Nucl. Mater. 239 (1996) 185.
[3] H. Matsui, D.S. Gelles, Y. Kohno, ASTM-STP 1125 (1992) 928.
[4] H. Matsui, H. Nakajima, S. Yoshida, J. Nucl. Mater. 205 (1993) 452.
[5] M. Kiritani, H. Takata, J. Nucl. Mater. 69&70 (1978) 227.
[6] T. Muroga, K. Araki, N. Yoshida, ASTM-STP 1047 (1990) 199.
[7] N. Yoshida, M. Kiritani, F.E. Fujita, J. Phys. Soc. Jpn. 39 (1975) 170.
[8] T. Hayashi, K. Fukumoto, H. Matsui, J. Nucl. Mater. 283–287 (2000) 234.
[9] K. Takahashi, H. Matsui, unpublished work.
[10] H. Matsui, H. Nakajima, The 1854th report of Institute for Material Research, 1991, p. 196.
[11] T. Hayashi, K. Fukumoto, H. Matsui, J. Nucl. Mater., these Proceedings.
[12] K. Nakai, C. Kinoshita, Y. Muroo, S. Kitajima, Philos. Mag. A 48 (1983) 215.